

Dispersion from an area source in the unstable surface layer: an approximate analytical solution

John D. Wilson

Department of Earth & Atmospheric Sciences, University of Alberta, Edmonton, Canada

*Correspondence to: J. D. Wilson, Department of Earth & Atmospheric Sciences, University of Alberta, 116 St. & 85 Ave., Edmonton, Alberta T6G 2E3, Canada. E-mail: jaydee.uu@ualberta.ca

An approximate solution to the advection-diffusion equation is given, applying to a plume in the unstably stratified surface layer emanating from a finite ground-level area source of trace gas. The approximation consists firstly of representing the mean wind profile by a power law, and secondly, in ‘splitting’ the governing equation so as to determine two components of the mean concentration that, in sum, satisfy the boundary conditions. The solution, which is easy to evaluate, is compared with numerical simulations using a standard Lagrangian stochastic trajectory model (LSM) and, provided the ratio of the upwind fetch of source to the Obukhov length is not too large ($|x/L| \lesssim 10$), agreement is very good. The Lagrangian model, in turn, is shown to be consistent with the Project Prairie Grass (PPG) dispersion data, subject only to the tuning of a flexible constant whose optimal value carries the implication that the ratio (S_c) of the eddy viscosity to the (far field) eddy diffusivity is not unity in the neutral limit, but rather $S_c \approx 0.64$. It seems unlikely this calibration results from having neglected deposition of the PPG ‘tracer’ (sulphur dioxide) to the surface.

Key Words: advection-diffusion equation; flux-gradient relationship; inverse dispersion; Lagrangian stochastic model; Project Prairie Grass; surface layer dispersion; turbulent dispersion; turbulent Schmidt number

Received 14 January 2015; Revised 5 May 2015; Accepted 16 June 2015; Published online in Wiley Online Library 09 September 2015

1. Introduction

The advection-diffusion paradigm no longer represents a fundamental framework for understanding or modelling turbulent dispersion, having long since been surpassed in generality by (e.g.) Lagrangian stochastic and large-eddy simulation models. Nonetheless, because it represents the only obvious prospect for an analytical description, the approach remains interesting, if for no other reason than from the perspectives of parsimony, and ease of evaluation. In the context of an ideal (i.e. stationary, horizontally homogeneous) atmospheric surface layer (ASL) the downwind (x) advection and vertical (z) dispersion of passive tracer is represented (approximately) by the advection-diffusion equation (ADE)

$$\bar{u} \frac{\partial \bar{c}}{\partial x} = \frac{\partial}{\partial z} \left(K_c \frac{\partial \bar{c}}{\partial z} \right), \quad (1)$$

where the profiles of (unidirectional) mean wind speed $\bar{u}(z)$ and of the eddy diffusivity $K_c(z)$ are appropriately given by Monin–Obukhov (MO) similarity theory. However, because Eq. (1) with MO profiles is intractable (even in the case of neutral stratification), all known exact solutions of Eq. (1) applicable in micrometeorology introduce a power-law representation

$\bar{u} = \bar{u}_H (z/H)^m$, $K_c = K_{cH} (z/H)^n$ for wind speed and eddy diffusivity, H being an arbitrary reference height. A solution for a surface line source originating (Monin and Yaglom, 1977) with O. F. T. Roberts (unpublished, circa. 1923) has subsequently been applied by many authors (e.g. van Ulden, 1978), and remains important as the basis for a working theory of the flux footprint (e.g. Horst and Weil, 1992, 1994; Kormann and Meixner, 2001). Philip’s (1959) analytical solution of Eq. (1) for a surface area source (given in Appendix C) was an early paradigm for quantifying local advection.

Another potential application for solutions of Eq. (1) is ‘inverse dispersion,’ whereby a theory for the relationship between the emission rate Q of a source and the mean concentration \bar{c} that results at a nearby point permits the former to be quantified by measuring the latter (e.g. Wilson *et al.*, 2012). This article has been motivated by a new flux estimation technique, loosely of the ‘flux-gradient’ type, in which the flux to the atmosphere from a small surface area source having known perimeter is deduced from the difference in line-averaged concentration (\bar{c}) along two slanting paths over the source. A flexible theory of the \bar{c} vs. Q relationship (or at least, $\partial \bar{c} / \partial z$ vs. Q) is needed to achieve the inversion for Q , and this article will provide a new solution to Eq. (1) that is convenient in that regard (complementing that of Philip (1959) as applied, for instance, by Wittich and Siebers, 2002).

By exploiting a suggestion of Shwetz (1949; see also Panchev *et al.*, 1971) and thereby retaining the MO profiles of (\bar{u}, K_c) , Wilson (1982a) gave an approximate solution of Eq. (1) for a finite ground-level area source in the stably (or neutrally) stratified surface layer. This was shown to agree with Lagrangian simulations and with experimental data, except near the outer edge of the concentration plume. Here, by the compromise of substituting the power law for wind speed (taking, in effect, a half-step towards the exact solutions alluded to above), a compact new approximate solution for unstable stratification is obtained (Appendix A gives a partial solution with the MO wind profile retained). The solution proves to be in reasonable agreement with the higher-fidelity Lagrangian stochastic (LS) treatment, whose implementation and whose consistency with observations will be discussed.

Section 2 gives the new solution and section 3 documents implementation of the LS model, whose agreement with the Project Prairie Grass observations is demonstrated in section 4. Finally section 5 compares the analytical and numeric (LS) solutions, along with the MO concentration profile which is in principle valid only *infinitely far downwind* from the leading edge of a source.

2. Solution to ADE with MO diffusivity and power-law wind

Defining $\Omega = -z_0/L$ where z_0 is the momentum roughness length and L the Obukhov length, the profiles adopted are

$$\bar{u} = \bar{u}_H (z/H)^m, \quad (2)$$

$$K_c = \frac{(k_v/S_c)u_*z}{\phi_c(z/L)}, \quad (3)$$

where

$$\phi_c = (1 + \beta \Omega z/z_0)^{-1/2} \quad (4)$$

(with $\beta = 16$) is the Dyer and Hicks (1970) formulation for the universal MO function representing the normalized concentration gradient, but for present purposes the Schmidt number S_c (ratio of the eddy viscosity to the eddy diffusivity in the neutral limit) will be permitted to differ from unity. In the convention adopted here the MO ϕ s take the value unity in the neutral limit, allowing potentially distinct von Kármán constants for momentum (k_v), heat (k_v/Pr , with Pr being the turbulent Prandtl number) and mass (k_v/S_c). The power law wind profile Eq. (2) reproduces the mean wind speed and wind shear at $z = H$ provided m, \bar{u}_H are specified as

$$m = \frac{\phi_m(H/L)}{k_v \bar{u}_H / u_*}, \quad (5)$$

$$\bar{u}_H = \frac{u_*}{k_v} \left[\ln \frac{H}{z_0} - \psi_m(H/L) + \psi_m(z_0/L) \right], \quad (6)$$

where here the MO functions are prescribed as

$$\psi_m(z/L) = 2 \ln \left\{ (1 + \phi_m^{-1})/2 \right\} + \ln \left\{ (1 + \phi_m^{-2})/2 \right\} - 2 \operatorname{atan}(\phi_m^{-1}) + \pi/2, \quad (7)$$

$$\phi_m(z/L) = (1 - \beta z/L)^{-1/4}, \quad (8)$$

which are Paulson's (1970) form for the mean wind profile and the Dyer–Hicks formulation for the MO dimensionless wind shear function ϕ_m .

Following Wilson (1982a), the problem is cast in dimensionless terms by introducing along-wind and vertical coordinates

$$\xi = \frac{x}{z_0}, \quad \lambda = \ln \frac{z}{z_0}. \quad (9)$$

(A displacement height d can be accommodated if $z - d$ is substituted throughout for the height z ; in principle the roughness length, say z_{0c} , for a scalar variable is distinct from z_0 , however in the context of an eddy diffusion solution the distinction can be overlooked). The mean concentration due to a finite upwind area source on ground is normalized as

$$\chi(\xi, \lambda) = \frac{u_* \bar{c}}{k_v Q}, \quad (10)$$

(the von Kármán constant $k_v = 0.4$ has been inserted in the denominator merely to uphold consistency with Wilson (1982a) and with earlier articles, e.g. Horst, 1979), and the corresponding (normalized) vertical flux density is

$$\frac{F}{Q} = -N \phi_c^{-1} \frac{\partial \chi}{\partial \lambda}, \quad (11)$$

where $N = k_v^2/S_c$.

With the chosen variables and profiles the advection-diffusion equation transforms to

$$e^{s\lambda} \frac{\partial \chi}{\partial \xi} = M \frac{\partial}{\partial \lambda} \left\{ (1 + \beta \Omega e^\lambda)^{1/2} \frac{\partial \chi}{\partial \lambda} \right\}, \quad (12)$$

where $s = 1 + m$ and

$$M = \frac{k_v}{S_c} \frac{u_*}{\bar{u}_H} \left(\frac{H}{z_0} \right)^m. \quad (13)$$

Following Shwetz's method, the solution is decomposed $\chi = \chi_0 + \chi_1$, where the components of the solution are required to satisfy

$$0 = M \frac{\partial}{\partial \lambda} \left[\phi_c^{-1}(\lambda, \Omega) \frac{\partial \chi_0}{\partial \lambda} \right], \quad (14)$$

$$e^{s\lambda} \frac{\partial \chi_0}{\partial \xi} = M \frac{\partial}{\partial \lambda} \left[\phi_c^{-1}(\lambda, \Omega) \frac{\partial \chi_1}{\partial \lambda} \right]. \quad (15)$$

At the top ($\lambda = \delta$, $z_\delta/z_0 = e^\delta$) of the concentration plume, $\chi_0 = \chi_1 = 0$, while at ground the height gradients are individually specified so as partition a unit surface tracer flux density as

$$r = -N \left(\phi_c^{-1} \frac{\partial \chi_0}{\partial \lambda} \right)_{\lambda=0}, \quad (16)$$

$$(1 - r) = -N \left(\phi_c^{-1} \frac{\partial \chi_1}{\partial \lambda} \right)_{\lambda=0}, \quad (17)$$

where a satisfactory choice for the flux partitioning factor r (≤ 1) is $r = 1/2$. The flux (r) 'carried' by χ_0 is height-independent. Therefore χ_1 is constrained such that the height gradient $\partial(\chi_0 + \chi_1)/\partial \lambda$ vanishes on $z = z_\delta$, ensuring that both concentration and vertical flux vanish along that surface (i.e. the top of the plume). The latter requirement yields a differential equation for the plume depth $\delta(\xi)$. By these steps one readily finds

$$\chi_0 = \frac{r}{N} \{B(\delta, \beta \Omega) - B(\lambda, \beta \Omega)\}, \quad (18)$$

where

$$B(x, \alpha) = \ln \left| \frac{\sqrt{1 + \alpha e^x} - 1}{\sqrt{1 + \alpha e^x} + 1} \right|. \quad (19)$$

(Recall χ_0 is the solution with tracer advection entirely neglected, so in fact Eq. (18) obtains irrespectively of whether one has adopted the MO profile or the power law for \bar{u}). Further steps

establish that the rate of growth of the plume with downwind distance is

$$\delta \equiv \frac{d\delta}{d\xi} = \frac{Ms}{r} \frac{\sqrt{1 + \beta\Omega e^\delta}}{e^{s\delta} - 1}, \quad (20)$$

and (integrating) the plume depth is given by the implicit equation

$$\frac{Ms}{r} \xi = B(0, \beta\Omega) - B(\delta, \beta\Omega) + (\beta\Omega)^{-s} \{A(1 + \beta\Omega e^\delta, m) - A(1 + \beta\Omega, m)\}. \quad (21)$$

The total concentration is found to be

$$\chi = \frac{1}{N(e^{s\delta} - 1)} \left\{ e^{s\delta} B(\delta, \beta\Omega) - e^{s\delta} B(\lambda, \beta\Omega) - (\beta\Omega)^{-s} A(1 + \beta\Omega e^\delta, m) + (\beta\Omega)^{-s} A(1 + \beta\Omega e^\lambda, m) \right\}. \quad (22)$$

In Eqs (21) and (22)

$$A(x, m) = \int \frac{(x-1)^m}{\sqrt{x}} dx = \frac{(x-1)^{m+1}}{(m+1)\sqrt{x}} + \sum_{i=1}^{\infty} \frac{(x-1)^{m+1+i}}{(m+1)\dots(m+1+i)} \frac{(2i-1)!!}{2^i x^{i+1/2}}, \quad (23)$$

where $i!!$ is the double factorial. (This integral does not appear to have been tabulated. Equation (23) captures the pattern that emerges from repeated integration by parts, and normally converges, proving in good agreement with a purely numerical evaluation. Appendix D outlines the code used).

The analytical solution also provides the spatial field of the vertical flux density, which (in normalized form) is

$$-N\phi_c^{-1} \frac{\partial\chi}{\partial\lambda} \equiv \frac{F(\xi, \lambda)}{Q} = \frac{e^{s\delta} - e^{s\lambda}}{e^{s\delta} - 1} \equiv \frac{z_\delta^s - z^s}{z_\delta^s - z^s}. \quad (24)$$

Interestingly (since $s = 1 + m$) the index m of the power law $\bar{u} \propto x^m$ controls the divergence of the vertical flux between the surface (where $F/Q = 1$) and the edge of the plume, a decay which is not linear. (The role of the eddy diffusivity is of course also involved in the control of plume depth.)

The neutral limit of the solution* is easily obtained by setting $\Omega = 0$ at the outset, but (reassuringly) it also emerges (albeit more laboriously) from the equations above. Under neutral stratification the plume depth is given by

$$\frac{Ms}{r} \xi = \frac{1}{s} (e^{s\delta} - 1) - \delta, \quad (25)$$

and the mean concentration is

$$\chi^N = \frac{e^{s\delta}}{N(e^{s\delta} - 1)} (\delta - \lambda) - \frac{1}{Ns} \frac{e^{s\delta} - e^{s\lambda}}{e^{s\delta} - 1}. \quad (26)$$

3. Lagrangian stochastic model

Lagrangian stochastic (LS) simulations will be taken as a criterion of accuracy for the analytical solution, once having (themselves) been tested (or rather, in effect, *calibrated*) against the Project Prairie Grass tracer point source dispersion trials. The LS model is well known and widely used, so that this section will stress *implementation*, rather than ancestry. Two codes were tested, and proved mutually consistent to within a margin that can probably be ascribed to their differing levels of discretization error.

3.1. Well-mixed, one-dimensional, first-order LS model

Lagrangian variables will be represented in upper case, viz. $W = dZ/dt$ is the vertical velocity of a particle or fluid element whose height is Z . A ‘first-order’ LS model explicitly computes particle velocity, while if it is to parallel the advection-diffusion equation (Eq. 1) it will neglect horizontal velocity fluctuations relative to the mean (\bar{u}), and (therefore) be qualified as being ‘one-dimensional’ (because only one *turbulent* velocity component is retained; for terminology and background on LS models see Thomson 1987; Wilson and Sawford 1996; Thomson and Wilson 2012). With the further approximation that the probability density function for the Eulerian vertical velocity fluctuations is a stationary Gaussian (with standard deviation σ_w), a unique algorithm for trajectories in the surface layer follows (in almost every respect) from the well-mixed condition (Thomson, 1987). The well-mixed 1D algorithm is

$$dX = \bar{u}(Z) dt, \quad (27)$$

$$dZ = W dt, \quad (28)$$

$$dW = a_w(Z, W) dt + \sqrt{C_0\epsilon(Z)} d\zeta, \quad (29)$$

where dt is the time step. In Eq. (29), a ‘generalized Langevin equation’, ϵ is the turbulent kinetic energy dissipation rate, C_0 is a dimensionless constant introduced by Kolmogorov, $d\zeta$ is a Gaussian random variate with zero mean and variance dt , and a_w , the deterministic part of the particle acceleration, is given by

$$a_w(Z, W) = \frac{-W}{\tau} + \sigma_w \frac{\partial\sigma_w}{\partial z} \left(1 + \frac{W^2}{\sigma_w^2} \right), \quad (30)$$

where

$$\tau = \frac{2\sigma_w^2}{C_0\epsilon} \quad (31)$$

is an effective Lagrangian decorrelation time-scale. In the limit of infinitesimal dt this model has the property that, applied to the motion of an ensemble of particles that are (already) well-mixed in an unbounded position-velocity space, it retains that distribution – the most powerful known constraint on this class of LS models. (Note: a *zeroth-order* LS model, i.e. the random Displacement Model or RDM, corresponds *exactly* with the advection-diffusion equation; Wilson and Yee, 2007 and Wilson, 2015.)

It is satisfying that the well-mixed condition establishes the rigour of a trajectory model, however in practice the time step is finite, typically specified $dt = \mu\tau$, with $\mu \ll 1$; and in consequence it is usually necessary to introduce an element that is extraneous to Thomson’s analysis, namely to avoid passage of trajectories beneath the chosen lower boundary (here, at $Z = z_0$) a reflection algorithm must be introduced. Wilson and Flesch (1993) proved that the well-mixed state is retained with perfect reflection if the turbulence is not only Gaussian, but in addition homogeneous – which is not the case here. Thus, implemented in (z, w, t) -space this algorithm entails two uncertainties, both minor for practical purposes, but needing to be flagged wherever (as here) the model is treated as a criterion for other solutions: (i) the reflection strategy *may* not be rigorous; and (ii) depending on the manner of solving Eqs (27)–(31), a bias may originate from the vertical inhomogeneity of turbulence properties, and in particular the time-scale τ .

3.2. Turbulence profiles adopted for the LS simulations

Wilson *et al.* (1981c) calibrated the above model (or rather, the equivalent model in (z^*, w_H, t_H) -space; Appendix B) against the Project Prairie Grass profiles of crosswind-integrated concentration at radial distance $x = 100$ from a continuous point

*The neutral limit proved consistent with the full solution (Eq. 22) evaluated with $\Omega = 10^{-6}$, which is about the smallest value attainable; at $\Omega = 10^{-8}$ a noticeable irregularity sets in.

source of gas, and recommended that the time-scale be specified as

$$\frac{2\sigma_w^2}{C_0\epsilon} \equiv \tau(z) = \frac{0.5z}{\sigma_w} \begin{cases} (1 - 6z/L)^{1/4}, & L < 0, \\ (1 + 5z/L)^{-1}, & L \geq 0. \end{cases} \quad (32)$$

This parametrization is combined with σ_w profiles

$$\sigma_w(z) = 1.25u_* \begin{cases} (1 - 3z/L)^{1/3}, & L < 0, \\ (1 + 0.2z/L), & L \geq 0 \end{cases} \quad (33)$$

(Kaimal and Finnigan, 1994). The mean wind speed is of course computed using Eqs. (6–8).

The above calibration is equivalent to a specification of the surface layer profiles of σ_w and of $\phi_\epsilon(z/L) \equiv k_v z \epsilon / u_*^3$, along with an auspicious tuning of the Kolmogorov constant C_0 . As discussed by Wilson *et al.* (2009), the value of C_0 implied by the above profiles is $C_0 \approx 3.1$. (Note: this differs from the value cited by Wilson *et al.* (2009) for a 1D model only because, here, the neutral ratio σ_w/u_* has been taken as $c_w = 1.25$, rather than 1.3.)

3.3. Implementation in (z, w, t) space

There are two elements to the LS model, namely, the computation of trajectories (i.e. implementation of an algorithm guided by the well-mixed condition) and the inference of concentration statistics from those trajectories. To the latter end a suitable range on the vertical axis was divided into bins of equal width in $\ln z/z_0$ and gridpoints equispaced in $\lambda \equiv \ln z/z_0$ were defined (and indexed ‘ k ’). Associated with each gridpoint, or rather layer, were upper and lower boundaries on the z/z_0 axis.

In each simulation, 19 sub-ensembles each of N_p paths were computed, with N_p of order 10^5 . (Breaking the ensemble into sub-ensembles, each featuring a different sequence of random numbers, allows to assign a standard error.) The time-step parameter μ was specified as $\mu = 0.01$. Particles were released at $X = 0, Z = z_0$ with a vertical velocity chosen randomly from the Gaussian PDF. Upon each time step dt the sequence of operations was:

1. compute needed velocity statistics and time step dt ;
2. update vertical velocity W , compute vertical step dZ ;
3. $Z \rightarrow Z + dZ/2$; then if $Z < z_0$,
 $Z \rightarrow 2z_0 - Z, W \rightarrow -W, dZ \rightarrow -dZ$;
4. store present position X as ‘ X_p ’, then step downwind:
 $X \rightarrow X + \bar{u}(Z) dt$;
5. if $X > x_{mx}$ (the desired fetch of area source), $X \rightarrow x_{mx}$ and
 $dX = x_{mx} - X_p$;
6. determine index k of the layer in which the particle resides;
7. increment accumulator $t_{res}(k)$ by the amount $dX/\bar{u}(Z)$;
8. repeat step 3.

The sub-ensemble normalized mean concentration \bar{c}/Q (after N_p paths) was derived as

$$\chi(k) = \frac{t_{res}(k)}{N_p \Delta z(k)}, \quad (34)$$

where $\Delta z(k)$ is the depth of the k th sampling layer, and then renormalized as $u_* \bar{c}/Q$ for comparison with PPG or as $u_* \bar{c}/(k_v Q)$ for comparison with the analytical solution. Because layers were very thin at small $z(k)$, it proved necessary to use double precision grid variables and accumulators.

An alternative implementation in ‘ (z_*, w_H, t_H) space’ is described in Appendix B (for the reasons given there). Happily, and as will be shown, the two implementations gave closely similar concentration fields.

3.4. Parametrization of gas absorption at the surface

Because the Project Prairie Grass measurements of the dispersion of sulphur dioxide serve here as the ultimate criterion for the analytical solution, and because Grynning *et al.* (1983) consider that surface absorption occurred during the PPG trials, some of the LS simulations to be shown have incorporated surface uptake.

It is relevant to note first of all that the PPG scientists concluded (Barad, 1958, p77) ‘there is no evidence of any significant loss of sulphur dioxide due to absorption by vegetation or any other factor.’ One of the lines of evidence supporting that statement was their ‘approximate check on’ the total SO_2 mass flux past their 100 m radius arc, which (though varying from run to run) tended to be within circa. 10% of their estimate of the emission rate Q , or better. Given that the horizontal mass flux estimates ignored the contribution of the eddy component (i.e. covariance of concentration fluctuations c' with fluctuations in horizontal wind speed), and in view of the relatively low spatial resolution of the summation performed to estimate the total flux, it is appropriate to interpret such a comment as meaning that deposition could be neglected as a good first approximation.

Suppose, then, one wished to estimate and represent surface uptake in simulations of the PPG trials. To the degree that it occurred, uptake of sulphur dioxide – to leaf and stalk surfaces and into the stomata of the sparse cover of grass, as well as to the soil – would have been modulated by many unreported elements of the prevailing circumstances: leaf area density, soil and plant moisture status, solar radiation, leaf surface contamination and/or wetness, and more. Surface uptake is universally parametrized in terms of a ‘deposition velocity’ w_d defined by co-located measurements of the depositional flux density $F(z_m)$ and a reference mean concentration $\bar{c}(z_m)$ at a reference height z_m assumed to lie within a constant flux layer,

$$w_d = \frac{F(z_m)}{\bar{c}(z_m)}. \quad (35)$$

The deposition resistance w_d^{-1} is regarded (Wesley and Hicks, 2000) as the series combination of an aerodynamic resistance

$$r_a = \int_{z_0}^{z_m} \frac{dz}{K_c(z)}, \quad (36)$$

along the aerial pathway from the roughness height to the reference height, a laminar surface sublayer diffusion resistance r_b (depending on surface geometry and the molecular diffusivity, at a minimum), and a complicated ultimate resistance r_c determined (depending on the nature of the canopy and substrate and the comprehensiveness of the treatment) by a combination of (for instance) stomatal and physiological resistances.

From the perspective of an LS model, only the contribution of $r_b + r_c$ needs to be parametrized, because trajectories to and from the roughness height z_0 are explicitly computed. This is most easily done by introducing a possibility for absorption (rather than reflection) each time a particle passes below $Z = z_0$, and Wilson *et al.* (1989) established that the needed reflection probability R is

$$\frac{1 - R}{1 + R} = \sqrt{\frac{\pi}{2}} \frac{w_d}{\sigma_w}, \quad (37)$$

where (at the surface) $\sigma_w = c_w u_*$ with $c_w = 1.25$. To parametrize absorption, each particle is given unit ‘mass’ upon its release, but each time it is subsequently reflected off the surface that mass is reduced (multiplicatively) by the factor R ; contributions of that particle to the concentration field are scaled by its mass.

Sehmel (1980) cites deposition velocities for sulphur dioxide over grass that span 0.002–0.02 m s^{-1} . Where the following LS

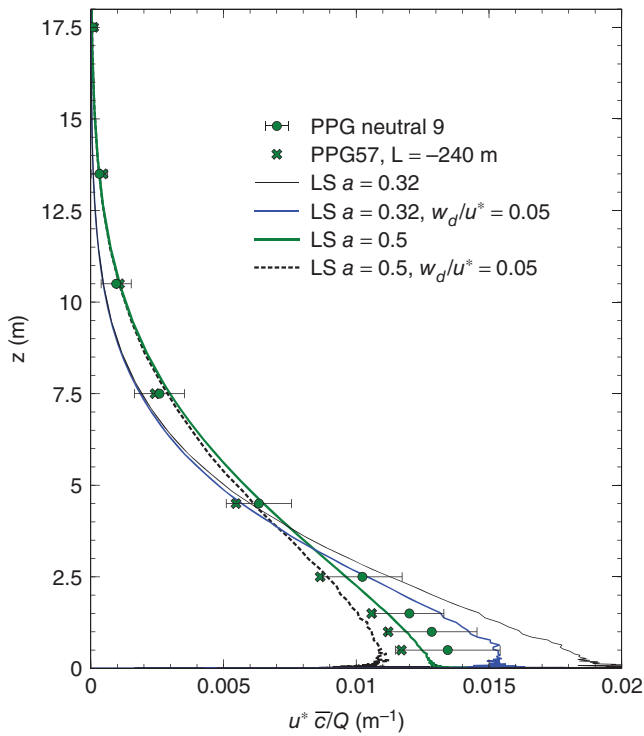


Figure 1. Comparison of Lagrangian stochastic simulations with Project Prairie Grass profiles (symbols) of crosswind-integrated concentration at radius $x = 100$ m from a point source, under neutral stratification.

simulations *have* included surface uptake – the default being that they have not – the value $w_d/u_* = 0.05$ used by Grynning *et al.* (1983) has been adopted, implying $R = 0.95$. This should not be interpreted as support for that particular value of the deposition velocity: rather, as will be seen, the simulations suggest that the deposition velocity was sufficiently small to have rendered deposition negligible, as originally surmised by the PPG scientists.

4. Validation of LS model against PPG

The LS model will serve (below) as criterion for the validity of the analytical solution, so we begin by ensuring that LS simulations are compatible with measurements. Figure 1 compares the LS simulations with the profile of crosswind integrated concentration measured at distance (radius) $x = 100$ m from the source in Project Prairie Grass trials, under nearly neutral stratification. Two representations of the PPG neutral profile have been given, viz. run 57 ($L = -240$ m, $z_0 = 0.0058$ m), and, the average and sample standard deviation from nine runs having $|L| \geq 50$ m. For this figure and others to follow LS simulations computed $19 \times 512\,000$ independent paths from the source (at $z_{src} = 0.46$ m), with time step $\Delta t/\tau = 0.01$; concentration was estimated by samplers equispaced in $\ln z$.

The far-field eddy diffusivity implied by the LS model in the neutral case is $K_\infty = ac_w u_* z$ such that the implied Schmidt number is $S_c = k_v/(ac_w)$. Figure 1 indicates that, as originally noted by Wilson *et al.* (1981c), the choice $a = 0.32$ (which implies $S_c = 1$) leads to poor agreement with PPG. In particular, in the height range from about $4 \leq z \leq 11$ m simulated concentrations are systematically too low, and this is not a deficiency that is amenable to correction by incorporating surface deposition – which could only further reduce those (simulated) concentrations.[†] What is needed, is to enhance the rate of vertical transport, and (again, in harmony with Wilson *et al.* 1981c)

[†]This deficit in the modelled concentration has the consequence that the total radial mass flux is underestimated relative to the known Project Prairie Grass source strength, as noted by Sawford (2001) and Wilson (2015).

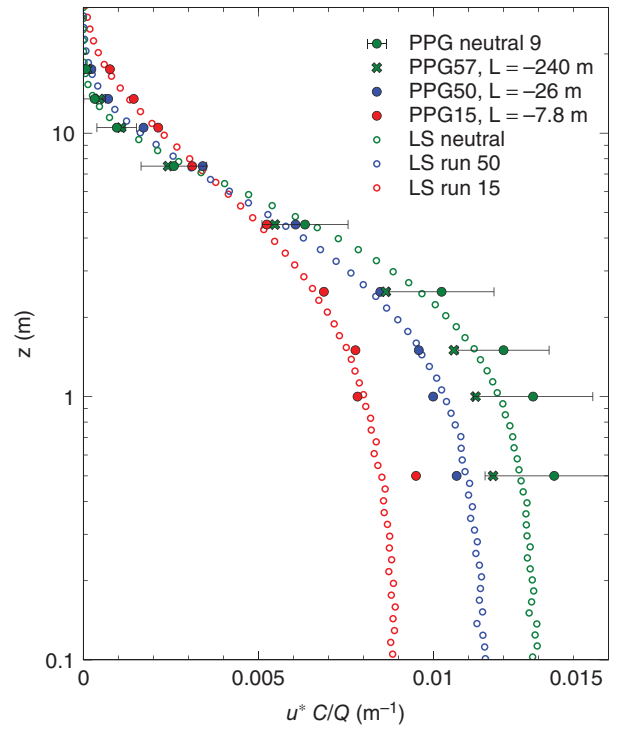


Figure 2. Project Prairie Grass profiles (solid circles) of crosswind-integrated concentration (at radius $x = 100$ m from a point source) in comparison with the Lagrangian stochastic (LS) simulations. The stratified PPG profiles are: run 50 (blue), $L = -26$ m and $z_0 = 0.0033$ m ($x/z_0 = 3.03 \times 10^4$); run 15 (red), $L = -7.8$ m and $z_0 = 0.003$ m ($x/z_0 = 3.33 \times 10^4$). LS solutions, open symbols.

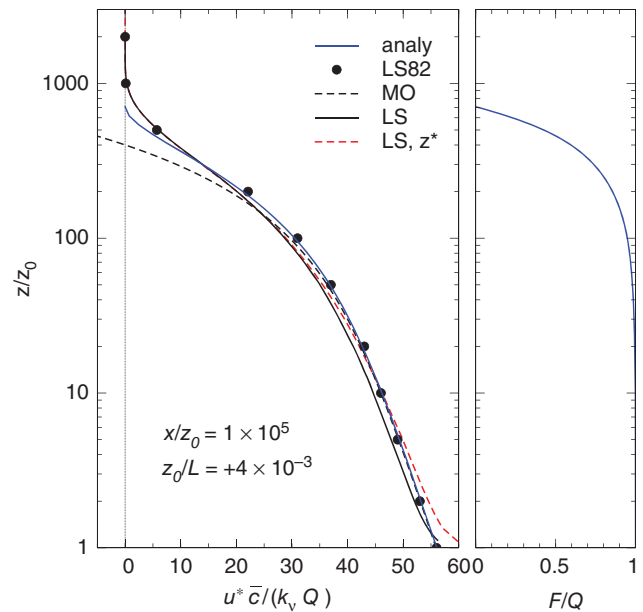


Figure 3. Normalized concentration and flux profiles at distance $x/z_0 = 10^5$ from the leading edge of a surface area source, in stable stratification ($z_0/L = 4 \times 10^{-3}$): comparison of the analytical solution (blue) with Lagrangian stochastic simulations (as tabulated by Wilson 1982b, and as recomputed here, red), and with the Monin–Obukhov profile (adjusted to fit surface concentration). (This is a case shown by Wilson, 1982a, his Figure 4.)

the calibration $a = 0.5$, implying $S_c = 0.64$, gives a satisfactory outcome. Figure 2 confirms that with $a = 0.5$ (and no deposition) the LS model also agrees very satisfactorily with Project Prairie Grass measurements made during moderately and strongly unstable stratification ($L = -28$ m, $L = -8$ m), while Figure 3 is an equally satisfactory outcome ($a = 0.5$, $w_d = 0$) for a case of stable stratification. (Note: Figure 3 pertains to an area source. LS simulations of PPG point source trials under stable stratification are shown by Wilson *et al.* 1981c, Figures 6, 7).

5. Performance of the analytical solution

This section will begin with a clarification of the extent to which one may *expect* the analytical solution and the Lagrangian simulation to coincide. The solution for $L \geq 0$, laid out in detail by Wilson (1982a), will be briefly revisited and confirmed, but the bulk of the results pertain to the unstable case. The analytical solution has invariably been evaluated with $N = k_v^2/S_c = 1/4$. Correspondingly the LS simulations use $k_v = 0.4$ and the above-documented formulation of $\sigma_w(z)$ and $C_0\epsilon(z)$, implying $C_0 \approx 3.1$ and $S_c \approx 0.64$.

5.1. Criterion for near-ground concentration profile

On first thought it would seem that, in view of the deepening constant-flux layer at the base of the plume off an area source, the correct concentration *gradient* near ground would be given by MO similarity theory (with appropriate allowance for one's choice of S_c), viz.

$$\frac{\partial \chi^{\text{MO}}}{\partial (z/z_0)} = - \left(\frac{u_* z_0}{k_v} \right) \left(\frac{\phi_c}{(k_v/S_c) u_* z} \right), \quad (38)$$

$$\frac{\partial \chi^{\text{MO}}}{\partial \ln(z/z_0)} = - \frac{\phi_c}{N}, \quad (39)$$

where $N = k_v^2/S_c$. Provided z/z_0 is not too large, the analytical solution, being based on the eddy-diffusion paradigm, should match this MO concentration gradient.

Further to that criterion, does the analytical solution correctly estimate the surface concentration? The latter is not provided by MO theory, which treats surface concentration (like surface temperature) as an external property. A convenient criterion here is the concentration profile given by the LS model; but in this context one must bear in mind that the LS model will (correctly) reveal the non-diffusive near field of the source, and thereby differ from the MO solution and the present analytic solution, at heights that are comparable with the turbulence length scale near the source. Of course, over natural surfaces one's specification of turbulence profiles as height $z \rightarrow 0$ is necessarily fictive, in that (inevitably) there exists an 'Unresolved Basal Layer' (Wilson and Flesch, 1993) in which velocity statistics cannot be (or have not been) measured, and because (anyway) the exact interpretation of the statement $z = z_0$ is ambiguous in that one cannot meaningfully assign an origin for the z axis. In the present simulations the length scale at $z = z_0$ is given as $z_0/2$, which is no more arbitrary than any other value one could reasonably have chosen. The point is that one may expect the LS model *not* to agree with Eq. (39) for small z/z_0 , because 'built in' to MO theory is an assumption that for $|z/L| \ll 1$ the eddy diffusivity $K_c \propto z$, and accordingly the mean concentration gradient plotted on a $\ln z$ coordinate is constant, in the limit of small $|z/L|$. (The effect of the near field of elevated sources is seen in the mean concentration profiles exhibited by Figure 2 of Wilson (1982b): very close to the level of the elevated area source the standard flux-gradient relationship does not apply, e.g. the mean flux runs against the mean gradient, just beneath the source).

5.2. The pre-existing solution for stable stratification

Recall that for the stable case, documented by Wilson (1982a), both the wind speed and eddy diffusivity are represented by MO profiles. Here it is only intended to affirm that the 1982 results are reproducible,[‡] and in that regard Figure 3 corresponds with Figure 4 of Wilson (1982a), the solution at distance $x/z_0 = 10^5$

[‡]The product δr on the second line of Wilson's (1982a) Eq. (21) ought to read $\delta \tau$.

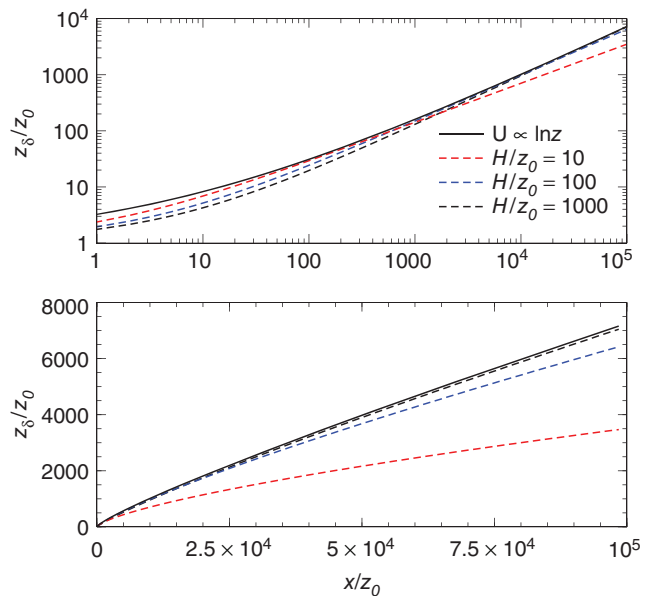


Figure 4. Analytical solutions for the depth z_δ of the plume versus downwind distance x/z_0 , under neutral stratification. H/z_0 refers to the reference height for solutions using the power-law wind profile: $H/z_0 = (10, 100, 1000)$.

from the leading edge of an area source, with $z_0/L = 4 \times 10^{-3}$. Though not shown by Wilson (1982a) the MO profile has also been plotted (with the Schmidt number adjusted to 0.64), its surface concentration having been assigned arbitrarily to line up with the analytical solution (of course the MO concentration profile entails a flexible surface concentration $\chi(z_0)$, and is 'unaware' of the finite extent of the source). Up to $z/z_0 \sim 10^2$ the slope of the MO profile accords very well with the analytical solution – as it should, within the growing constant-flux layer at the base of the concentration plume.

On Figure 3 two Lagrangian solutions are shown, in addition to that tabulated by Wilson (1982b) and which was plotted on Figure 4 of Wilson (1982a). Readers will notice that the 1982 solution appears to lack the deviation (as $z/z_0 \rightarrow 1$) from the MO profile slope manifested by the other LS solutions. As covered above, such a deviation is *expected*. The inconsistency stems from the fact that the 1982 solutions entailed a larger level of statistical error than contemporary solutions (for which standard error was too small to plot): limited computing power restricted the number of paths it was feasible to compute, such that it was necessary to smooth the profile at small z/z_0 . In doing so, the author had (wrongly) assumed there would be no significant deviation from the constant $\partial \chi / \partial \ln z$ slope. That anomaly aside, results proved closely consistent with Wilson (1982a) over all combinations of $(x/z_0, z_0/L \geq 0)$ that were examined.

5.3. Influence of the choice of reference height

The compromise of adopting the power-law mean wind profile carries the penalty that one cannot correctly represent the MO wind profile at all heights. The impact of the unconstrained parameter H (reference height) can be gauged by Figure 4, which plots the plume depth for neutral stratification as per Eq. (25; power law wind) alongside that which stems from the use of the semi-logarithmic wind profile (Wilson, 1982a, Eq. 24N). As can be expected, the power-law solution is sensitive to the prescription of H , such that if a small value is used then plume depth differs greatly at large x/z_0 from the preferred solution. However at fetches liable to be of interest ($1 \ll x/z_0 \ll 10^5$) it can be expected that any choice $H/z_0 \gg 10$ should return an adequate profile of concentration near ground, or more specifically, within the developing constant-flux layer.

5.4. Unstable stratification: performance of the new solution

For the following results, unless otherwise stated, the reference height for the wind profile was specified as $H/z_0 = 100$ and the A function (Eq. 23) was evaluated out to 200 terms. Where plotted, the MO concentration profiles are

$$\chi^{\text{MO}} = \chi^{\text{MO}}(z_0) - \frac{1}{k_v^2/S_c} \left\{ \ln \frac{z}{z_0} - \psi(z, L) + \psi(z_0, L) \right\}, \quad (40)$$

where

$$\psi = \psi(\phi_c) = 2 \ln \left\{ \frac{1}{2} (1 + \phi_c^{-1}) \right\}, \quad (41)$$

with ϕ_c given by Eq. (4). The surface concentration $\chi^{\text{MO}}(z_0)$ has been assigned arbitrarily to permit comparing the concentration gradients across solutions. (Recall the scaling in use here, i.e. $\chi = u_* \bar{c}/(k_v Q)$, which explains the k_v^2 factor in Eq. 40).

Figure 5 compares the analytical solution with the LS model, for the case $x/z_0 = 5 \times 10^3$, $z_0/L = -10^{-3}$. The analytical solution (not greatly differing if H/z_0 is increased by more than an order of magnitude) and the MO curve are in excellent agreement over the bulk of the plume, but this does not undercut the utility of the analytical solution because contrary to the MO curve it accounts for the finite fetch, and thereby pins down the surface concentration that lies outside the scope of the MO profile, as well as the decaying gradient near the top of the plume. One point needing clarification is that even well above $z = z_0$ there is a slight difference between the slope $\partial \chi / \partial \ln z$ of the LS solution and the (matching) gradients of the analytical solution and the MO profile. This is readily understandable. The far-field diffusivity implied by the LS model is $\sigma_w^2 \tau$ where the chosen profiles (Eqs. 32 and 33) imply that for $L \leq 0$

$$\sigma_w^2 \tau = (k_v/S_c) u_* z (1 - 6z/L)^{1/4} (1 - 3z/L)^{1/3}, \quad (42)$$

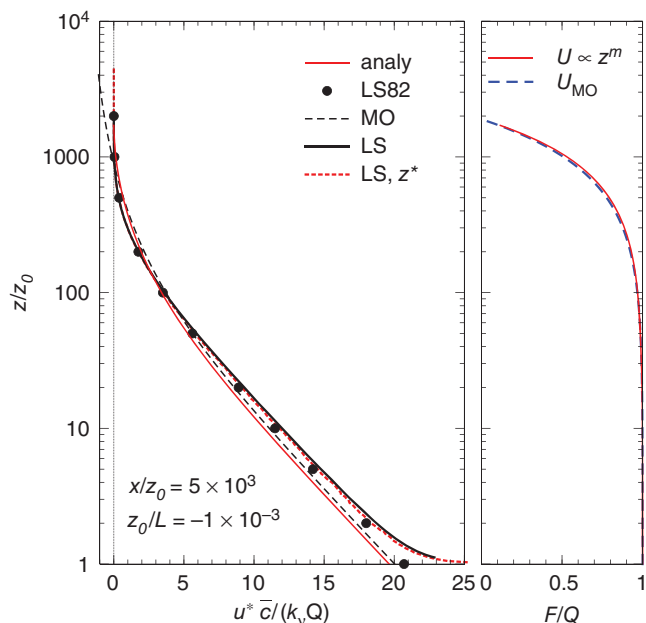


Figure 5. Normalized concentration and flux profiles at distance $x/z_0 = 5 \times 10^3$ from the leading edge of a surface area source in unstable stratification ($z_0/L = -1 \times 10^{-3}$): comparison of the analytical solution with Lagrangian stochastic solutions, and with the Monin-Obukhov profile (adjusted to fit surface concentration by imposing $u_* \chi / (k_v Q) = 20$). LS solutions include: (i) the tabulated LS solution of Wilson (1982b), computed using the z^* method; and contemporary LS calculations of paths in (ii) (z, w, t) -space (solid black line) and (iii) in (z_*, w_H, t_H) -space (dashed red line). The flux profile corresponding to the (incomplete) analytical solution with Monin-Obukhov wind profile (blue dashed line) is given in Appendix A.

which differs from the MO eddy diffusivity (evaluated according to Eq. (4), the Dyer and Hicks (1970) formulation with an explicit adjustment of S_c) which is:

$$K_c = \frac{(k_v/S_c) u_* z}{\phi_c(z/L)} = (k_v/S_c) u_* z (1 - \beta z/L)^{1/2}. \quad (43)$$

Evidently the two formulations differ in their z/L dependence, and readers may wonder why the profiles chosen for the LS simulations were not chosen for *exact* compatibility with (say) the Dyer–Hicks far-field eddy diffusivity. The reason is that it is the nature of the Lagrangian model that one requires specific profiles for σ_w and for τ (or equivalently ϵ).

Figure 5 also gives the analytic solution for the profile of the normalized vertical flux, and in particular, compares Eq. (24) – the present solution (with $U \propto z^m$) – against the solution given by retaining the MO wind profile (Eq. A9). The near coincidence of the two flux profiles suggests that the penalty for invoking the power law wind profile is not severe, a point we return to below.

Figures 6 and 7 give the analytical solution for $z_0/L = -10^{-3}$ at $x/z_0 = (2 \times 10^3, 2 \times 10^4)$, respectively using a logarithmic and a linear height axis; the summation in Eq. (23) was truncated at 100 terms for the longer fetch. Recall that the context here is the case of finite fetch of ground-level (area) source, for which the constant flux layer does not (in general) extend to the top of the ASL. It would appear from the results that one might just as well base a flux-gradient method on the MO profile, notwithstanding that it (by definition) presupposes an infinite fetch (or equivalently, the existence a constant flux layer to all heights of interest, i.e. to the top of the surface layer). However when the MO profile and the present *fetch-cognizant* solution are plotted using a linear height axis (Figure 7) it can be seen that accounting for the finite fetch will give a superior estimate.

These points are clearer when one focuses on the height gradient of concentration. From Eq. (24) it is evident that

$$\frac{\partial \chi}{\partial (z/z_0)} = - \left(\frac{u_* z_0}{k_v} \right) \left(\frac{\phi_c}{(k_v/S_c) u_* z} \right) \left(\frac{z_\delta^5 - z^5}{z_\delta^5 - z_0^5} \right), \quad (44)$$

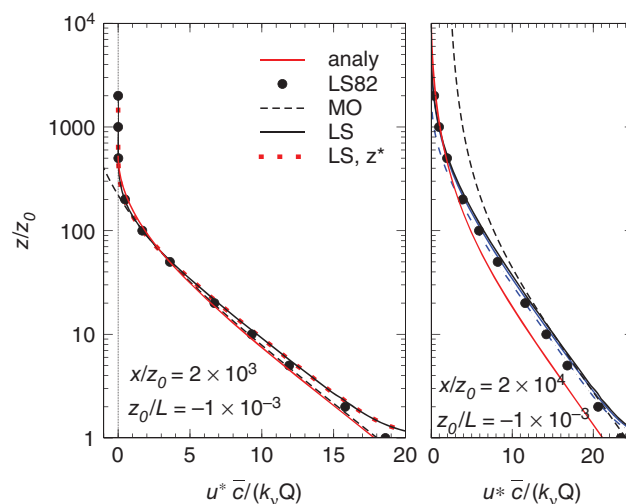


Figure 6. Normalized concentration profiles at distances $x/z_0 = (2 \times 10^3, 2 \times 10^4)$ from the leading edge of a surface area source, in the unstably stratified surface layer ($z_0/L = -10^{-3}$). Solid red lines give the present analytical solution (power-law wind profile and MO eddy diffusivity); solid circles tabulate the solution given by Wilson (1982b) based on a well-mixed LS model, which is shown in comparison with new LS solutions (solid black, and red dashed lines) as described here. The black dashed line is the MO concentration profile for a constant flux layer (i.e. it is appropriate to the situation of an infinite fetch of source) with an arbitrary offset on the concentration axis. On the right-hand panel the solution using the z_* implementation is not shown; blue lines are LS simulations using the power-law wind profile (solid, $H/z_0 = 10^3$; dashed, $H/z_0 = 10$; please note that the solid blue line overlaps the solid black line, i.e. the LS solution with MO wind profile).

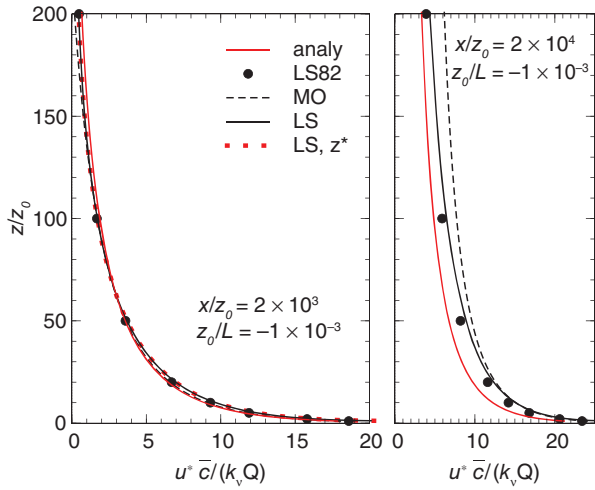


Figure 7. Normalized concentration profiles at distances $x/z_0 = (2 \times 10^3, 2 \times 10^4)$ from the leading edge of a surface area source, in the unstably stratified surface layer ($z_0/L = -10^{-3}$): details as for Figure 6, but using a linear height axis.

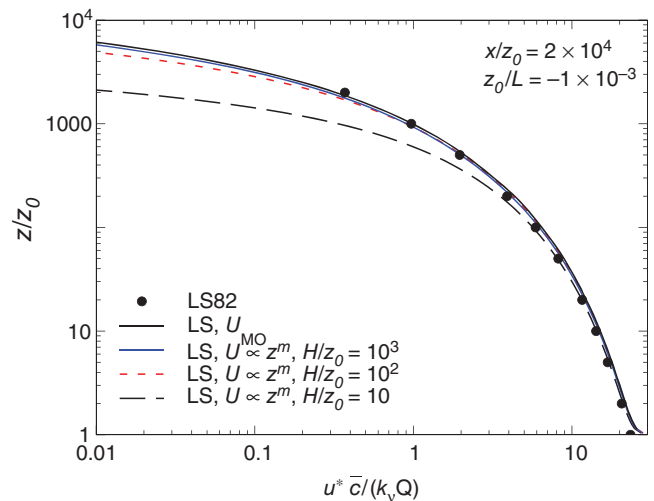


Figure 9. Comparative LS simulations with the MO wind profile and the power law wind profile: concentration profile at distance $x/z_0 = 2 \times 10^4$ from the leading edge of a surface area source ($z_0/L = -10^{-3}$).

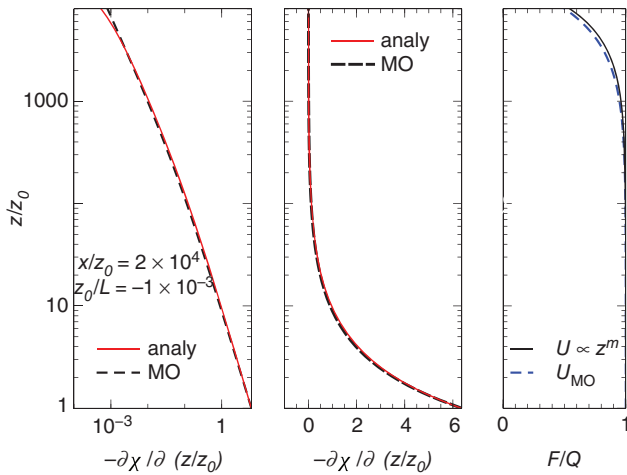


Figure 8. Profiles of the normalized concentration gradient and vertical flux at distance $x/z_0 = 2 \times 10^4$ from the leading edge of a surface area source ($z_0/L = -10^{-3}$). For power law profiles, $H/z_0 = 100$. Analytic flux profiles from Eq. (24), power law wind, and retaining the MO wind profile (Appendix A).

where the first factor on the right-hand side juggles the units, the second is the reciprocal of the eddy diffusivity (in its dimensional form, for clarity), and the final factor attenuates the flux with increasing distance from the source. The corresponding MO gradient is of course Eq. (38), and so we may write

$$\frac{\partial \chi}{\partial(z/z_0)} = \frac{\partial \chi^{\text{MO}}}{\partial(z/z_0)} \left(\frac{z_\delta^s - z^s}{z_\delta^s - z_0^s} \right). \quad (45)$$

Figure 8 plots $\partial \chi / \partial(z/z_0)$ and the normalized vertical flux density for $z_0/L = -10^{-3}$ at fetch $x/z_0 = 2 \times 10^4$. It is interesting to note that one must plot $\partial \chi / \partial(z/z_0)$ on a log axis in order to distinguish the difference in slope relative to the infinite fetch (MO) case, suggesting that assumption of the MO profile for the purpose of making flux-gradient measurements of area source fluxes ought to be very forgiving in terms of the necessary fetch.

Returning now to Figures 6 and 7, two further points may be made. Firstly, note that the concentration profiles provided by the two implementations of the LS model are very consistent (i.e. they overlap), albeit slightly different from that of the 1982 tabulation (probably for the reason given earlier), and with their gradient slightly different from the MO gradient (again, for the reason given above). Secondly, deviation between the analytical and LS solutions is greater for the longer of the two fetches (right hand panel). Short of adjusting the β parameter of the K_c

profile – which would be hard to justify – there seems no remedy within the compass of the present solution.

5.5. Sources of error in the analytic solution

It is of interest to establish the relative importance of two sources of error in the analytic solution, viz. that which stems from the adoption of a power law wind profile, and that which arises from, or is inherent to, the Shwetz solution procedure.

Error of the first type can be examined without reference to the analytic solution, by comparing LS simulations using the MO wind profile (i.e. identical in every respect to those shown above) with those that result when the power law formulation is substituted. Figure 9 suggests that (for that particular fetch and stability) the impact of invoking the power law representation is greatest near the upper edge of the plume, and more serious for smaller choices of H/z_0 , the reference height: relative to the LS simulation with the MO wind profile, simulations with the power law wind profile underestimate the plume depth. However in this case, simulations with $U \propto (z/H)^m$ and $H/z_0 = 10^3$ differ negligibly from the reference solution (LS with MO wind profile) and this establishes that provided due care is taken in the choice of H/z_0 , the dominant source of error in the *analytic* solution is of the second type, i.e. that which arises because the solution χ does not exactly satisfy the advection-diffusion equation. A further indication that use of the power law wind profile is the less serious source of error is implied by the near coincidence (Figure 5) of two flux profiles both stemming from the Shwetz solution procedure, one (Eq. 24) based on the the power law wind profile and the other (Eq. A9) based on a MO wind profile.

But if a power law representation of the wind profile is an acceptable compromise, then what of the eddy diffusivity profile? – for with *both* parametrized by power laws, we have exact solutions to the ADE. Figure 10 plots Philip’s (1959) *exact* solution for a surface area source (with $\bar{u} \propto z^m$, $K_c \propto z^n$; Appendix C) alongside the new solution (of section 2) for which $\bar{u} \propto z^m$ but $K_c \propto z/\phi_c(z/L)$. Evidently one’s specification of the reference height H is considerably more consequential for the Philip solution than for the present (new) solution. As it has been established that solutions are not unduly sensitive to the reference height where the power law is introduced *for wind speed alone*, one must conclude this heightened sensitivity to H (of Philip’s solution relative to that of section 2) is a consequence of having invoked the power law *for eddy diffusivity*. This implies that the shape (i.e. $K_c \propto z/\phi_c(z/L)$) of the MO profile for eddy diffusivity is less amenable to an approximation of power law form than is the shape of the mean wind profile.

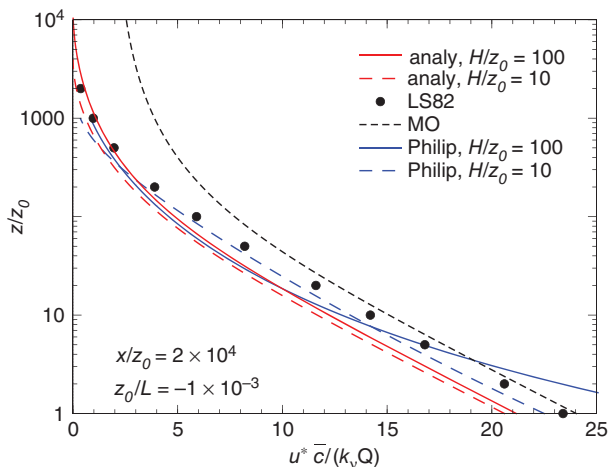


Figure 10. Normalized concentration profiles at distance $x/z_0 = 2 \times 10^4$ from the leading edge of a surface area source, in the unstably stratified surface layer ($z_0/L = -10^{-3}$). Red lines give the present analytical solution (power-law wind profile and MO eddy diffusivity); solid circles tabulate the solution given by Wilson (1982b) based on a well-mixed LS model. The black dashed line is the MO concentration profile for a constant flux layer (i.e. it is appropriate to the situation of an infinite fetch of source) with an arbitrary offset on the concentration axis. Blue lines give Philip’s (1959) analytical solution with $H/z_0 = (10, 100)$.

6. Conclusions

Retaining the MO profile for the eddy diffusivity, this article extends to unstable stratification an approximate analytical solution to the advection diffusion equation given by Wilson (1982a). The necessity to adopt a power law representation of the mean wind for the $L < 0$ case has the consequence of introducing an arbitrary choice (the reference height H), but solutions are not unduly sensitive to reasonable choices of the latter. Furthermore retention of the MO diffusivity is advantageous because solutions to the ADE that invoke a power law representation for the latter (i.e. for K_c as well as for wind speed) are more sensitive to the specification of the non-physical and arbitrary reference height.

Notwithstanding the arbitrariness of Shwetz’s decomposition of the advection-diffusion equation, the solution proves useful for the surface area source, as judged by its close agreement with the LS model (and by implication, according to Figures 1 and 2, with reality). Of course the Lagrangian model handles a much wider range of problems, so that strictly speaking one has no need of eddy diffusion solutions, however there are circumstances where a simple formula is preferred. Wilson and Flesch (2016) apply this solution in the context of a modified flux-gradient technique for determining ground/air exchange fluxes, based on pairing line-averaged concentrations along upward- and downward-slanting paths over a finite surface area source; this is a case for which the inversion (to obtain the flux from the concentration difference) by conventional means (viz. the LS model ‘WindTrax’, Wilson *et al.*, 2012) is computationally cumbersome, owing to the need to compute trajectories from a sufficient number of heights to adequately represent the slanting gas sample-paths.

The Schmidt number, or another parameter equivalent to it, has been made explicit both in the analytical solution and the Lagrangian solution, and their mutual consistency does not hinge on any adjustment in that regard. Should it eventually be proven (contrary to what has been assumed here) that the neutral Schmidt number for passive tracer $S_c = 1$, as many readers may already believe on the evidence of the classic flux-gradient experiments,[§] then the utility of the analytical solution is not diminished: one

[§]However Wilson (2013) gives an indication that those experiments are not as definitive on the matter as could be wished. Independently of the inference drawn in this article from the Project Prairie Grass trials, numerous tracer dispersion studies (summarized by Harper *et al.* 2010, Table A1) have shown

simply recalibrates S_c (and a or C_0 in the LS model) to whatever value later evidence recommends.

Acknowledgement

This work has been supported by a grant from the Natural Sciences and Engineering Research Council of Canada.

Appendix A

Partial solution with MO diffusivity and MO wind

The goal of this work had been to obtain a solution to the advection-diffusion equation (Eq. 1) that would be applicable for unstable stratification, with appropriate MO profiles of wind speed and eddy diffusivity: section (2), a solution with the MO diffusivity but a power law wind profile, represents only a half step in that direction. The solution procedure of Shwetz promptly leads to difficult integrals if one adopts the Paulson wind profile (or the alternative proposed by Wilson 2001), however a partial solution (plume depth; the field of the vertical flux density) has been obtained with the wind profile represented as

$$\frac{\bar{u}}{u_*} = \frac{1}{k_v} \left\{ \ln \frac{z}{z_0} - 2 \ln \frac{1 + \sqrt{z/(-L)}}{1 + \sqrt{z_0/(-L)}} \right\}, \tag{A1}$$

which follows from specifying the MO function for the normalized mean wind shear as

$$\phi_m = \left(1 + \sqrt{z/(-L)} \right)^{-1}. \tag{A2}$$

Figure A1 indicates that Eq. (A1) is in satisfactory agreement with the wind profile computed using widely accepted choices for ϕ_m (viz. Dyer and Hicks, 1970; Dyer and Bradley, 1982).

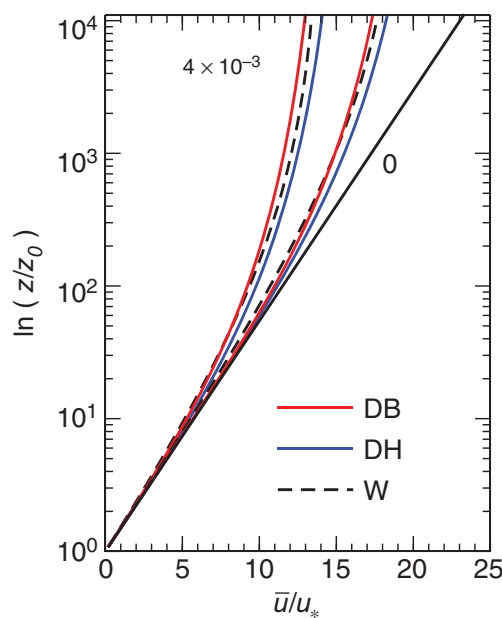


Figure A1. Comparison of Eq. (A1) (W) for the mean wind profile in unstable stratification ($z_0/|L| = 0, 4 \times 10^{-4}, 4 \times 10^{-3}$) versus profiles based on the $\phi_m(z/L)$ functions recommended by Dyer and Hicks (1970; DH) and by Dyer and Bradley (1982; DB).

With Eq. (A1) for $\bar{u}(z)$ along with the conventional MO eddy diffusivity (Eq. 3), the advection-diffusion equation

that emission rates Q yielded by inverse dispersion on the basis of the assumption $S_c \approx 0.64$ agree well with the true release rate.

transforms to

$$e^\lambda \{ \lambda - \psi(\lambda, \Omega) \} \frac{\partial \chi}{\partial \xi} = N \frac{\partial}{\partial \lambda} \left\{ \phi_c^{-1}(\lambda, \Omega) \frac{\partial \chi}{\partial \lambda} \right\}, \quad (\text{A3})$$

where ϕ_c is given by Eq. (4) and

$$\psi = 2 \ln \frac{1 + \sqrt{\Omega e^\lambda}}{1 + \sqrt{\Omega}}, \quad (\text{A4})$$

with $\Omega = -z_0/L$ and (as before) $N = k_v^2/S_c$. Now working through the Shwetz procedure one finds the slope of the plume to be

$$\delta = \frac{(1 + \beta \Omega e^\delta)^{1/2} N/r}{G(\delta)} \quad (\text{A5})$$

where the function $G(t)$ is

$$G(t) = te^t - 2(e^t - \Omega^{-1}) \ln \frac{1 + \sqrt{\Omega e^t}}{1 + \sqrt{\Omega}} + 2\Omega^{-1/2} (1 - e^{t/2}). \quad (\text{A6})$$

To express the result

$$\frac{N}{r} \int d\xi = \int \frac{G(\delta) d\delta}{\sqrt{1 + \beta \Omega e^\delta}} + \hat{c}_2 \quad (\text{A7})$$

of integrating Eq. (A5) term by term, define $\theta(\delta) = \Omega e^\delta$, $\Theta(\delta) = \beta \Omega e^\delta$. Then with the help of various transformations of the variable of integration one finds that the plume depth δ at distance ξ from the leading edge of the source can be obtained by solving

$$\begin{aligned} \frac{N}{r} \xi = & \frac{2}{\beta \Omega} \left\{ \sqrt{1 + \Theta} (\ln \Theta - 2) - 2 \ln \left(\frac{\sqrt{1 + \Theta} - 1}{\sqrt{\Theta}} \right) \right\} \\ & - \frac{2 \ln(\beta \Omega)}{\beta \Omega} \sqrt{1 + \Theta} + \frac{4}{\beta \Omega} \ln(1 + \sqrt{\Omega}) \sqrt{1 + \Theta} \\ & - \frac{4}{\sqrt{\beta} \Omega} \left\{ \frac{\ln(1 + \sqrt{\theta})}{\sqrt{\theta}} + \ln \left(\frac{1 + \sqrt{\theta}}{\sqrt{\theta}} \right) \right\} \\ & - \frac{4}{\sqrt{\beta} \Omega} (1 + \sqrt{\theta}) \left\{ \ln(1 + \sqrt{\theta}) - 1 \right\} \\ & + \frac{2}{\sqrt{\Omega}} \left\{ 1 - \frac{\ln(1 + \sqrt{\Omega})}{\sqrt{\Omega}} \right\} \ln \left(\frac{\sqrt{1 + \Theta} - 1}{\sqrt{1 + \Theta} + 1} \right) \\ & - \frac{2}{\sqrt{\beta} \Omega} \ln \left\{ 1 + 2\Theta + 2\sqrt{\Theta(1 + \Theta)} \right\} + \hat{c}_2. \quad (\text{A8}) \end{aligned}$$

To obtain this result, two terms have been simplified by the approximation that, with $\beta = 16 \gg 1$, $\beta + 1 \approx \beta$. The integration constant \hat{c}_2 was evaluated by forcing Eq. (A8) to coincide with the neutral solution (Wilson's 1982 Eq. 24N) at a 'calibration point,' i.e. a small value of the plume depth such that buoyancy effects should have had negligible impact. As a check on the analytical solution for $\delta(\xi)$, Eq. (A5) has also been integrated numerically by a Runge-Kutta method, using the neutral form to provide δ directly at small ξ (e.g. in the region $\Omega e^\delta = z_\delta/|L| \leq 2 \times 10^{-3}$).

Due to the difficulty of the final integration, the concentration field for the area source has not been obtained, however the vertical flux density (i.e. flux field for an area source) is given by

$$f_u(\xi, \lambda) = 1 - \frac{G(\lambda)}{G(\delta)}. \quad (\text{A9})$$

Figures 5 and 8 indicate that this flux profile agrees closely with that of section (2).

Appendix B

Implementation of LSM in (z_*, w_H, t_H) space

There was cause to wonder whether the LS calculations according to section 3.3 might have been compromised by the 'Δt bias error' identified by Wilson and Flesch (1993), and/or by the surface reflection algorithm, which lies outside the scope of Thomson's (1987) well-mixed condition. Therefore it was useful to also implement the formulation of Wilson *et al.* (1981c), whereby particle motion in the real world is mapped into a system of sheared homogeneous turbulence. (Later discussion of this approach, by Wilson *et al.* 1983 and Thomson 1984, addressed the equivalent process in (x, z, t) space; but it appears that, subsequent to Wilson *et al.* (1981c), there is no report of trajectories having been computed in this 'zstar-system'.)

The reasoning that culminated in (or justifies) the model will not be reiterated here, but it bears mention that the algorithm was subsequently proven to be well-mixed, and indeed equivalent to the *unique* well-mixed model given above. In this section we will slightly adjust the terminology of Wilson *et al.* so that Lagrangian variables are in upper case. Let H be a reference height in the surface layer (note: the H of this section is unrelated to the reference height for the power-law wind profile of the analytical solution, and its specification is entirely free) at which vertical velocity fluctuations are characterized by a standard deviation σ_{wH} and integral time-scale τ_H . Position increments on the z_* axis are given by

$$dZ_* = (W_H + \bar{W}) dt_H, \quad (\text{B1})$$

where \bar{W} is a bias velocity

$$\bar{W} = \sigma_{wH} \tau(z) \frac{\partial \sigma_w}{\partial z}, \quad (\text{B2})$$

and W_H is stochastic with variance σ_{wH} and time-scale τ_H . The stochastic component is conveniently computed by the Langevin equation

$$dW_H = -\frac{W_H}{\tau_H} dt_H + \sigma_w \sqrt{2dt_H/\tau_H} r, \quad (\text{B3})$$

where r is a standardized Gaussian random variate (zero mean, unit variance).

The relationship between z_* and real height z is given by

$$\frac{dz}{dz_*} = \frac{\sigma_w(z) \tau(z)}{\sigma_{wH} \tau_H}, \quad (\text{B4})$$

and (depending on the choice of σ_w and τ profiles) this may be amenable to analytical integration. With the choices used here, the relationship is of the same form as the MO mean wind profile; for stable stratification

$$(1 + 5H/L) \frac{z_*}{H} = \ln \frac{z}{z_0} + 5 \frac{z - z_0}{L} \quad (\text{B5})$$

while for unstable stratification the relationship is analogous to Eqs (6)–(8), viz.

$$\frac{z_*}{H(1 - \beta_\tau H/L)^{1/4}} = \ln \frac{z}{z_0} - \psi_\tau(z/L) + \psi_\tau(z_0/L), \quad (\text{B6})$$

where

$$\psi_\tau(z/L) = 2 \ln \left[(1 + \phi_\tau^{-1})/2 \right] + \ln \left[(1 + \phi_\tau^{-2})/2 \right] - 2 \operatorname{atan}(\phi_\tau^{-1}) + \pi/2, \quad (\text{B7})$$

$$\phi_\tau(z/L) = (1 - \beta_\tau z/L)^{-1/4}, \quad (\text{B8})$$

(in which $\beta_\tau = 6$). Finally, motion along the horizontal axis occurs with a transformed velocity, i.e.

$$dX = \bar{u}(Z) \frac{\tau(z)}{\tau_H} dt_H. \quad (\text{B9})$$

For any wanted fetch x_{mx} of source a suitable upper limit to the z/z_0 axis was chosen, and the corresponding value of z_* was divided into N_k layers (typically $N_k = 201$). The turbulent component of the motion is homogeneous on the z_* axis, but the bias component and the horizontal distance step refer back to z -space. Accordingly, arrays were created, these being indexed to the z_* layers, and storing the horizontal distance step $dX(k)$ and the bias velocity $\bar{W}(k)$. Paths were computed with $dt_H/\tau_H = \mu = 0.05$.

Apart from its computational rapidity, this model has the virtue that trajectories need not be reflected at the lower boundary (note: $z = z_0$ maps to $z_* = 0$). One simply allows the particle's (transformed) height Z_* to evolve as it will, reversing (only) the bias velocity whenever $Z_* < 0$. Whenever the index k is wanted, it is based on $|Z_*|$, and if $|Z_*|$ is such as to imply $k > N_k$ one sets $k = N_k$. On each step a concentration accumulator is incremented,

$$\Delta_x(k) = \Delta_x(k) + dX(k) \quad (\text{B10})$$

and sub-ensemble normalized mean concentration (after N_P paths, and here showing the u_*/k_v factor included in comparisons with the analytical solution) is

$$\chi(k) = \frac{u_* \Delta_x(k)}{k_v N_P \Delta z(k) \bar{u}(k)}. \quad (\text{B11})$$

Again, it proved vital to define the axes and the layer boundaries and thicknesses, as well as the concentration accumulators, using double precision arithmetic. The order of operations was the same as that given above.

Appendix C

Philip's exact solution of the ADE

Philip (1959) gave an exact solution to Eq. (1) with power law profiles

$$\bar{u} = \bar{u}_H (z/H_u)^m = \mathcal{U} z^m, \quad (\text{C1})$$

$$K_c = K_{cH} (z/H_K)^n = \kappa z^n, \quad (\text{C2})$$

valid provided $n \neq 1$ (i.e. neutral stratification is excluded). Just as indicated earlier in regard to (m, \bar{u}_H) , one may choose (n, K_{cH}) to reproduce the eddy diffusivity⁹ and its height gradient at the reference height. For computations shown here $H \equiv H_u \equiv H_K$ and:

$$n = 1 - \frac{H}{\phi_c(H/L)} \left[\frac{\partial \phi_c(z/L)}{\partial z} \right]_{z=H}, \quad (\text{C3})$$

$$K_{cH} = \frac{(k_v/S_c) u_* H}{\phi_c(H/L)}, \quad (\text{C4})$$

with

$$\phi_c = \begin{cases} (1 - 16z/L)^{-1/2} & , z/L < 0 \\ 1 + 5z/L & , z/L > 0. \end{cases} \quad (\text{C5})$$

⁹There is no necessity to enforce the constraint $n = 1 - m$ (Schmidt's conjugate power law) that is obligatory if parameterizing the eddy viscosity for the constant stress layer.

Philip introduces the dimensionless variable

$$\eta = \frac{\mathcal{U} z^r}{r^2 \kappa x} \quad (\text{C6})$$

where $r = 2 + m - n$, and his solution for the mean concentration due to a unit area source at the surface covering $x \geq 0$ is

$$\bar{c}(x, \eta) = \frac{1}{(1-n)\Gamma(\mu)\kappa} \left(\frac{r^2 \kappa x}{\mathcal{U}} \right)^{1/\beta} F(\eta, \beta) \quad (\text{C7})$$

where $\mu = (1+m)/r$, $\beta = r/(1-n) \equiv 1/(1-\mu)$, and

$$F(\eta, \beta) = 1 - \Gamma(\mu) \eta^{1/\beta} + \frac{\eta}{\beta-1} - \frac{\eta^2}{2!(2\beta-1)} + \frac{\eta^3}{3!(3\beta-1)} - \frac{\eta^4}{4!(4\beta-1)} + \dots \quad (\text{C8})$$

For large η this series approximation for $F(\eta, \beta)$ does not converge, however (as stated by Philip) for the η range liable to be of interest convergence is rapid.

Appendix D

Evaluation of $A(x, m)$

$A(x, m)$ is defined by Eq. (23). Suppose the infinite sum is evaluated out to N terms. Symbolically, $A(x, m, N)$ can be evaluated as follows, 'dblfcrl' being the double factorial of its argument:

```
s=1+m; xm1=x-1;
A=pow(xm1, s) / s*1/sqrt(x);
for(i=1; i<=N; ++i) {
  ireal=(double) i;
  sequence=s;
  for(k=1; k<=i; ++k) {
    kreal=(double) k;
    sequence=sequence*(s+kreal);
  }
  term=pow(xm1, s+ireal) / sequence*dblfcrl(2*i-1);
  term=term*1.0/pow(2, ireal)*1/pow(x, ireal+0.5);
  A=A+term;
}
return(A);
```

References

- Barad ML. 1958. *Project Prairie Grass, a Field Program in Diffusion*, 1. Technical Report Geophysical Research Papers No. 59, TR-58-235(1). Air Force Cambridge Research Center: Bedford, MA.
- Dyer AJ, Bradley EF. 1982. An alternative analysis of flux-gradient relationships at the 1976 ITCE. *Boundary-Layer Meteorol.* **22**: 3–19.
- Dyer AJ, Hicks BB. 1970. Flux-gradient relationships in the constant flux layer. *Q. J. R. Meteorol. Soc.* **96**: 715–721.
- Gryning SA, van Ulden AP, Larsen S. 1983. Dispersion from a continuous ground-level source investigated by a K model. *Q. J. R. Meteorol. Soc.* **109**: 355–364.
- Harper LA, Flesch TK, Weaver KH, Wilson JD. 2010. The effect of biofuel production on swine farm methane and ammonia emissions. *J. Environ. Qual.* **39**: 1984–1992.
- Horst TW. 1979. Lagrangian similarity modeling of vertical diffusion from a ground-level source. *J. Appl. Meteorol.* **18**: 733–740.
- Horst TW, Weil JC. 1992. Footprint estimation for scalar flux measurements in the atmospheric surface layer. *Boundary-Layer Meteorol.* **59**: 279–296.
- Horst TW, Weil JC. 1994. How far is far enough? The fetch requirements for micrometeorological measurement of surface fluxes. *J. Atmos. Oceanic Technol.* **11**: 1018–1025.
- Kaimal JC, Finnigan JJ. 1994. *Atmospheric Boundary-Layer Flows*. Oxford University Press: Oxford, UK.
- Kormann R, Meixner FX. 2001. An analytical footprint model for non-neutral stratification. *Boundary-Layer Meteorol.* **99**: 207–224.
- Monin AS, Yaglom AM. 1977. *Statistical Fluid Mechanics*. MIT Press: Cambridge, MA.

- Panchev S, Donev E, Godev N. 1971. Wind profile and vertical motions above an abrupt change in surface roughness and temperature. *Boundary-Layer Meteorol.* **2**: 52–63.
- Paulson CA. 1970. The mathematical representation of wind speed and temperature profiles in the unstable atmospheric surface layer. *J. Appl. Meteorol.* **9**: 857–861.
- Philip JR. 1959. The theory of local advection. *J. Meteorol.* **16**: 535–547.
- Sawford BL. 2001. 'Project Prairie Grass – a classic atmospheric dispersion experiment revisited'. In *14th Australasian Fluid Mechanics Conference*, 10–14 December 2001, Adelaide. <http://people.eng.unimelb.edu.au/imarusic/proceedings/14/FM010206.PDF> (accessed 17 July 2015).
- Sehmel G. 1980. Particle and gas dry deposition: a review. *Atmos. Environ.* **14**: 983–1011.
- Shwetz M. 1949. On the approximate solution of some boundary layer problems. *Appl. Math. Mech.* **13**: 257–266 (in Russian).
- Thomson DJ. 1984. Random walk modelling of diffusion in inhomogeneous turbulence. *Q. J. R. Meteorol. Soc.* **110**: 1107–1120.
- Thomson DJ. 1987. Criteria for the selection of stochastic models of particle trajectories in turbulent flows. *J. Fluid Mech.* **180**: 529–556.
- Thomson DJ, Wilson JD. 2012. History of the Lagrangian stochastic model for turbulent dispersion. In *Lagrangian Models of the Atmosphere, Geophysical Monograph*, Lin J, Brunner D, Gerbig C, Stohl A, Luhar A, Webley P. (eds.) **200**: 19–36. American Geophysical Union: Washington, DC.
- van Ulden AP. 1978. Simple estimates for vertical diffusion from sources near the ground. *Atmos. Environ.* **12**: 2125–2129.
- Wesley ML, Hicks BB. 2000. A review of the current status of knowledge on dry deposition. *Atmos. Environ.* **34**: 2261–2282.
- Wilson JD. 1982a. An approximate analytical solution to the diffusion equation for short-range dispersion from a continuous ground-level source. *Boundary-Layer Meteorol.* **23**: 85–103.
- Wilson JD. 1982b. Turbulent dispersion in the atmospheric surface-layer. *Boundary-Layer Meteorol.* **22**: 399–420.
- Wilson DK. 2001. An alternative function for the wind and temperature gradients in unstable surface layers. *Boundary-Layer Meteorol.* **99**: 151–158.
- Wilson JD. 2013. Turbulent Schmidt numbers above a wheat crop. *Boundary-Layer Meteorol.* **148**: 255–268.
- Wilson JD. 2015. Computing the flux footprint. *Boundary-Layer Meteorol.* **156**: 1–14, doi: 10.1007/s10546-015-0017-9.
- Wilson JD, Flesch TK. 1993. Flow boundaries in random flight dispersion models: Enforcing the well-mixed condition. *J. Appl. Meteorol.* **32**: 1695–1707.
- Wilson JD, Flesch TK. 2016. Generalized flux-gradient technique pairing line-average concentrations on vertically separated paths. Manuscript submitted for publication to *Agric. For. Meteorol.*
- Wilson JD, Sawford BL. 1996. Review of Lagrangian stochastic models for trajectories in the turbulent atmosphere. *Boundary-Layer Meteorol.* **78**: 191–210.
- Wilson JD, Yee E. 2007. A critical examination of the Random Displacement Model of turbulent dispersion. *Boundary-Layer Meteorol.* **125**: 399–416.
- Wilson JD, Thurtell GW, Kidd GE. 1981c. Numerical simulation of particle trajectories in inhomogeneous turbulence. III. Comparison of predictions with experimental data for the atmospheric surface-layer. *Boundary-Layer Meteorol.* **21**: 443–463.
- Wilson JD, Legg BJ, Thomson DJ. 1983. Calculation of particle trajectories in the presence of a gradient in turbulent velocity variance. *Boundary-Layer Meteorol.* **27**: 163–169.
- Wilson JD, Ferrandino FJ, Thurtell GW. 1989. A relationship between deposition velocity and trajectory reflection probability for use in stochastic Lagrangian dispersion models. *Agric. For. Meteorol.* **47**: 139–154.
- Wilson JD, Yee E, Ek N, d'Amours R. 2009. Lagrangian simulation of wind transport in the urban environment. *Q. J. R. Meteorol. Soc.* **135**: 1586–1602 (see also Erratum, *QJRMS* Vol. 136, Notes & Correspondence).
- Wilson JD, Flesch TK, Crenna BP. 2012. Estimating surface-air gas fluxes by inverse dispersion using a backward Lagrangian stochastic trajectory model. In *Lagrangian Models of the Atmosphere*, Geophysical Monograph, Lin J, Brunner D, Gerbig C, Stohl A, Luhar A, Webley P. (eds.) **200**: 149–161. American Geophysical Union: Washington, DC.
- Wittich K-P, Siebers J. 2002. Aerial short-range dispersion of volatilized pesticides from an area source. *Int. J. Biometeorol.* **46**: 126–135.